



# Optimization and kinetic study of biodiesel production from *Jatropha curcas* oil in supercritical methanol environment using ZnO/ $\gamma$ -Al<sub>2</sub>O<sub>3</sub> catalyst

Zeliha Derya Ceran<sup>1</sup> · Velid Demir<sup>1</sup> · Mesut Akgün<sup>1</sup>

Received: 10 October 2023 / Revised: 30 December 2023 / Accepted: 8 January 2024  
© The Author(s) 2024

## Abstract

In this study, the conversion of crude *Jatropha curcas* oil into biodiesel through transesterification was investigated in the presence of heterogeneous solid catalysts under supercritical methanol environment. The principal impetuses catalyzing the expansion in optimal biodiesel production are primarily attributed to the increasing demand for sustainable energy sources, the availability of raw materials, and innovations in production methodologies. To maintain the optimization, 6 wt% and 10 wt% of zinc oxide (ZnO) were incorporated into gamma-alumina ( $\gamma$ -Al<sub>2</sub>O<sub>3</sub>) through a wet impregnation method followed by calcination at 900 °C. Furthermore, the study examined the effect of alcohol/oil molar ratio, reaction temperature, and reaction time on the process to achieve maximum biodiesel production. The study revealed that a catalyst consisting of 10 wt% ZnO on  $\gamma$ -Al<sub>2</sub>O<sub>3</sub> exhibited exceptional performance with a biodiesel yield of 95.64% under the reaction conditions of a molar ratio of 1:40 oil to methanol, a temperature of 300 °C, a pressure of 9 MPa, and a residence time of 3 min compared to the yield of 100% under same condition at residence time of 9 min. After thorough investigation, the kinetics of the catalytic transesterification reaction were elucidated, and suitable kinetic parameters were proposed.

**Keywords** Biodiesel · Heterogeneous catalyst · *Jatropha curcas* · Supercritical methanol · Transesterification · Zinc oxide

## 1 Introduction

Nowadays, due to the rapidly increasing population worldwide, the consumption of fossil fuel energy is increasing day by day, which increases the need and demand for more profitable alternative renewable energy [1]. Among all other alternative fuels, biodiesel as a blend of fatty acid alkyl esters is a fuel that is attracting significant interest and studies due to its biodegradability, non-toxicity, and production from organic sources [2]. The most common and effective method to obtain biodiesel is trans-esterification. Biodiesel can be derived from vegetable oil, animal fat, and algae oil with short-chain alcohol such as methanol. Since the production of biodiesel is mainly based on the trans-esterification of biological oils, it reduces carbon dioxide emissions on a

large scale, which makes it environmentally friendly [3, 4]. Adding an excess of alcohol facilitates shifting the equilibrium of the reaction towards esters, as acceleration of the reaction can be achieved by using a catalyst when the reaction reaches equilibrium. Although homogeneous alkaline catalysis, such as sodium hydroxide or potassium hydroxide, is preferred as it allows the reaction to occur approximately 4000 times faster than acid catalysis and leads to higher efficiency with lower temperature and pressure, it presents some problems to processing different feedstocks such as inedible oils with high free fatty acid (FFA) content. In this regard, the problem of soap formation can cause a decrease in the content of the final product along with a difficult separation process. Thus, different alternative catalysts are developed in order to eliminate the disadvantages caused by these catalysts [5, 6]. The abovementioned drawbacks give priority to the application of heterogeneous catalysts due to their reusability, non-corrosive properties, ease of separation, lower cost, energy savings, enhanced fatty acid alkyl ester yield, and biodiesel purity, as well as its high tolerance to water and FFAs in the feedstocks [7]. According to Ramos et al. [8], drawbacks of heterogeneous catalysis

✉ Mesut Akgün  
akgunm@yildiz.edu.tr

<sup>1</sup> Department of Chemical Engineering, Faculty of Chemical and Metallurgical Engineering, Yildiz Technical University, Davutpasa Campus, Esenler, Istanbul 34220, Turkey

in transesterification reactions encompass lower conversion rates that may necessitate more rigorous reaction conditions compared to homogeneous catalysis, as well as mass transfer resistance resulting from the presence of three phases (oil, alcohol, and catalyst) in the reaction mixture. Furthermore, base catalysts utilized in this process can be adversely affected by elevated FFA and water content.

To date, the trans-esterification under supercritical alcohol technology plays an essential role by promoting higher yields of biodiesel at shorter reaction times compared to conventional esterification methods which require hours. A supercritical condition occurs when the temperature and pressure of a fluid are above their critical points. In this regard, methanol and ethanol at critical temperatures of 239.3 °C and 240.8 °C and critical pressures of 8.1 MPa and 6.3 MPa, respectively, are the most common alcohols used in this technique [9–12]. On the other hand, the use of edible vegetable oils and animal fats as feedstock for biodiesel production has become a controversial issue due to competition with the food industry. With the high demand for vegetable oil as a food source, it is necessary to consider that its use as a fuel is not justified. Accordingly, non-edible oils such as *Jatropha curcas* can make a significant contribution to the production of biodiesel [13]. *Jatropha curcas* seeds contain a large amount of active ingredients ranging from 27 to 40% such as phorbol esters, trypsin inhibitors, phytates, lectins, and saponins [14, 15]. Furthermore, the presence of phorbol esters and curcins in *Jatropha* indicates the incompatibility of the oil with the properties of oils classified as edible, which means that *Jatropha* oil is a promising option for biofuel production [16]. To justify the use of inedible vegetative feedstock for biodiesel production, it is essential to consider the overall environmental and economic benefits of biofuels compared to fossil fuels. While there are concerns about resource competition, biofuels offer several advantages, including lower greenhouse gas emissions, reduced dependence on imported fossil fuels, and potential economic benefits for rural communities. Overall, while the use of inedible vegetative oil for biodiesel production has the potential to compete with natural resources for food production, it is essential to balance the benefits and drawbacks of biofuels and ensure that they are produced sustainably and equitably.

Studies demonstrate that *Jatropha curcas* seed oil contains high levels of oleic (C18: 1) and linoleic acids (C18: 2) approximately 43.32% and 36.70% respectively, which may vary slightly by region [17]. In this study, biodiesel production was carried out under different reaction conditions using a catalyst synthesized by zinc oxides (ZnO) over  $\gamma$ -Al<sub>2</sub>O<sub>3</sub> with 10% weight loading, using wet impregnation method followed by calcination at 900 °C. To investigate the catalytic performance of the catalyst, reactions were carried out in a continuously operating packed bed reactor

(PBR) to produce biodiesel from crude *Jatropha* oil (CJCO) by trans-esterification under supercritical methanol environment. The reactions were carried out at 3 different temperatures of (260, 280, and 300 °C) with other parameters of oil to methanol molar ratios of (1:20, 1:25, 1:30, 1:35, and 1:40) and reaction times (1, 3, 5, 7, and 9 min), where the reaction pressure was constant at 9 MPa. Moreover, the reaction kinetic model was proposed for this study and the re-usability of the catalyst was also examined. The novelty and uniqueness of this work are attributed to the fact that it yields exceptionally high biodiesel outputs in a remarkably short timeframe, surpassing the results reported in existing literature. This will be elaborated upon in the following. The authors strongly recommend stopping on the review that synthesizes the results of multiple investigations focused on developing heterogeneous catalysts utilizing a diverse range of waste, natural, or commercial materials under supercritical conditions of alcohols [7]. These types of studies serve as a valuable resource for comprehending the current state of the field and identifying promising avenues for further exploration.

## 2 Material and methods

### 2.1 Materials

*Jatropha curcas* oil was obtained by hydraulically pressing the seeds in Sudan. Methanol as a reaction medium (99%) was from Merck, Germany. Zinc(II) nitrate hexahydrate (98%) was from Sigma-Aldrich, Germany, and  $\gamma$ -aluminum oxide (1/8" pellets) was from Alfa Aesar, Germany.

### 2.2 Catalysts preparation

The ZnO/ $\gamma$ -Al<sub>2</sub>O<sub>3</sub> syntheses were performed using the "Incipient wetness impregnation" method. A total of 10% w/v of the Zn was provided from Zn(NO<sub>3</sub>)<sub>2</sub>·6H<sub>2</sub>O and mixed with deionized water at ambient temperature. Subsequently, the homogeneous solution was added to  $\gamma$ -Al<sub>2</sub>O<sub>3</sub> pellets by 1:1 volume ratio. The sample was impounded in an ultrasonic water bath for 2 h to provide diffusion of zinc oxide into the carrier ( $\gamma$ -Al<sub>2</sub>O<sub>3</sub>) and left to dry in an oven at 105 °C for 2 h to completely remove water. Activation of the catalyst was performed by calcining the catalyst in a muffle oven at 900 °C for 4 h. In some cases, lower catalyst loadings such as 6 wt% may be preferred due to reducing the amount of catalyst required for a given reaction volume. Lower catalyst loadings can also reduce the overall cost and environmental impact of the process. However, it is important to note that lower catalyst loadings may also result in lower reaction rates or yields, particularly for feedstocks with high levels of FFAs as they were calculated to be equivalent to 22.9%

according to American Oil Chemists Society (AOCS) official method Ca 5a-40 (notably, no reaction was implemented to lower the oil's FFA content and it was utilized in its original state during the transesterification process in a supercritical methanol environment). In these cases, higher catalyst loadings may be necessary to ensure complete conversion and minimize the risk of side reactions. This highlights the importance of considering the FFA content of feedstocks when selecting appropriate catalyst loadings for transesterification processes. The decision to use a calcination temperature of 900 °C for 4 h as the basis for catalyst preparation was carefully considered. To illustrate this point, during the calcination process, a sample of catalyst loading was subjected to a temperature of 700 °C for a duration of 4 h. X-ray diffraction (XRD) analysis was subsequently performed on these samples. However, the resulting XRD patterns did not exhibit prominent peaks corresponding to the catalyst, indicating low crystallinity. Considering this, the calcination conditions for the ZnO/ $\gamma$ -Al<sub>2</sub>O<sub>3</sub> catalyst were optimized to ensure complete crystallization of ZnO, stability of  $\gamma$ -Al<sub>2</sub>O<sub>3</sub>, and complete removal of water and organic compounds from the catalyst through calcination at 900 °C for 4 h. These conditions result in a highly active and durable catalyst.

### 2.3 Catalyst characterization

The synthesized nanoparticles were checked by X-ray diffraction (XRD) using PANalytical X'Pert PRO model conducted with a Cu anode,  $\lambda = 1.54059 \text{ \AA}$ ) which were accelerated at 45 kV and 40 mA over  $2\theta$  angle range of  $10^\circ$ – $80^\circ$ . The Fourier-transform infrared (FTIR) (Thermo Fisher Scientific–Nicolet iS 10, USA) spectra of the samples were recorded in the wavenumber range of 400 to 4000  $\text{cm}^{-1}$ . Sample preparation was carried out by the KBr method. Scanning electron microscopy (SEM) equipped with energy-dispersive spectroscopy (EDS) analysis (SEM–EDS model Zeiss EVO® LS 10) was used to analyze the morphology of the nanoparticles. The specific surface area ( $S_{\text{BET}}$ ) was determined by the Brunauer–Emmett–Teller (BET) method (Quantachrome Quadrasorb SI).

### 2.4 Biodiesel production

The above synthesized and characterized catalyst was positioned to fill the volume of the PBR. The inner tube of the reactor has a diameter of 1.5 cm and a length of 12.9 cm. Two high-pressure pumps were used to pump Jatropha oil and methanol through separate feed lines, which pass through a preheater zone before reaching the reactor. Feed streams quickly reach the reactor conditions while passing through the preheating section. The temperature inside the reactor was controlled using the PID controller, and the sensor was installed inside a muffle. The temperature process variable (PV) was viewed through the PID control display according to the experiment set point (SP). On the other hand, the pressure was monitored and controlled using the manual back pressure regulator. A mixture of biodiesel and glycerol was cooled by a heat exchanger, samples were collected, and the fatty acid methyl ester content was calculated (Fig. 1). The highest FAME contents from the different experimental conditions were analyzed using a Perkin Elmer Autosystem XL GC, with software version (6.3.2.0646). The biodiesel yield was calculated according to Eq. (1) [18].

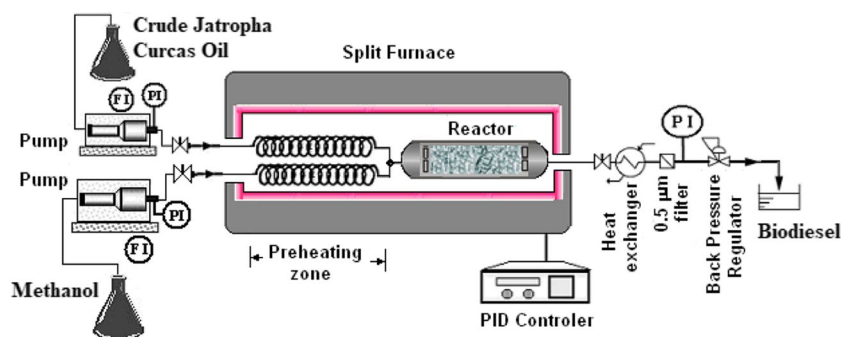
$$\text{Biodiesel Yield (\%)} = \frac{\text{Weight of biodiesel obtained (g)}}{\text{Weight of oil reacted (g)}} \times 100 \quad (1)$$

Moreover, the residence times at supercritical conditions in the reactor were calculated according to Eq. (2).

$$\tau = \frac{V_{\text{void}}}{F_{\text{MeOH}} \cdot \frac{\rho_{\text{feed-MeOH}}}{\rho_{\text{Sc-MeOH}}(T,P)} + F_{\text{oil}} \cdot \frac{\rho_{\text{feed-oil}}}{\rho_{\text{oil}}(T,P)}} \quad (2)$$

where  $V_{\text{void}}$  is the reactor void volume;  $\rho_{\text{Sc}}(P,T)$  and  $\rho_{\text{feed}}$  are the fluid densities in  $\text{g mL}^{-1}$  under reaction conditions and at feed pump conditions, respectively; and  $F_{\text{MeOH}}$  and  $F_{\text{oil}}$  are the volumetric flow rates in  $\text{mL min}^{-1}$  of MeOH and oil, respectively.  $\rho_{\text{oil}}(P,T)$  is estimated using GCVOL Group Contribution Method according to reaction conditions [19]. The densities of MeOH in elevated temperatures and pressures were estimated using Peng–Robinson Equation of State (PR–EoS). PR–EoS and the same in terms of density are given in Eqs. 3 and 6, respectively [20].

**Fig. 1** Schematic representation of catalytic biodiesel production in supercritical methanol environment



$$P = \frac{RT}{V-b} - \frac{a \cdot \alpha(T)}{V(V+b) + b(V-b)} \quad (3)$$

$$a = \frac{0.45724 \cdot (RT_c)^2}{P_c}, b = \frac{0.07780 \cdot RT_c}{P_c} \text{ and } \alpha(T) = \left[ 1 + K \left( 1 - \sqrt{T/T_c} \right) \right]^2 \quad (4)$$

$$K = 0.37464 + 1.54226 \cdot \omega - 0.26992 \cdot \omega^2 \quad (5)$$

$$(b^3P + b^2RT - ab)\rho^3 - (3b^2P + 2bRT - a)\rho^2 + (bP - RT)\rho + P = 0 \quad (6)$$

where  $a$  and  $b$  are generalized functions of critical temperature, critical pressure, and acentric factor ( $\omega$ ). The real root obtained by solving Eq. (6) gives the density of MeOH at reactor conditions.

## 3 Results and discussion

### 3.1 Fatty acid components of CJCO

The contents of fatty acid components in CJCO were achieved by quantitative GC–MS (Elite-5 ms Capillary Column—30 m × 0.25 mm I.D. × 0.25 μm). Helium was used as carrier gas with a flow rate of 1.30 mL/min at different temperatures. Based on the quantitative GC–MS analysis, it was found that oleic acid was the highest fatty acid component in CJCO, accounting for approximately 43.25% of the total fatty acid content (see Table 1). This is in line with previous studies that have reported high levels of oleic acid in *Jatropha curcas* oil [21, 22]. Most of the remaining fatty acid components identified in CJCO include palmitic acid (13.93%), stearic acid (6.46%), linoleic acid (32.25%), and linolenic acid (0.12%). These findings suggest that CJCO has a high potential as a renewable source of oleic acid, which is widely used in biodiesel production.

**Table 1** CJCO fatty acid components

Fatty acid	Content (%)
Myristic acid (C14:0)	0.06
Palmitic acid (C16:0)	13.93
Palmitoleic acid (C16:1)	0.74
Stearic acid (C18:0)	6.46
Oleic acid (C18:1)	43.25
Linoleic acid (C18:2)	32.25
Arachidic acid (C20:0)	0.27
Linolenic acid (C18:3)	0.12

## 3.2 Catalyst characterization

### 3.2.1 Scanning electron microscopy

The surface morphology of the catalyst was investigated using SEM technique. The SEM images of bare  $\gamma$ -Al<sub>2</sub>O<sub>3</sub> pellets revealed coarse rock/sand-like shapes (Fig. 2a), which facilitated the loading of ZnO particles. After calcination, the SEM image of the ZnO/ $\gamma$ -Al<sub>2</sub>O<sub>3</sub> (10 wt%) catalyst showed agglomerated particles (Fig. 2b). This morphological change was attributed to the sintering of ZnO particles during calcination.

The formation of active sites over the catalyst surface due to the loading of ZnO resulted in more effective catalytic performance, as confirmed by the experimental results. Another notable feature observed in the SEM images was the presence of porous structures on the surface of calcined catalyst, which could provide additional active sites for reactant adsorption and reaction. These porous structures were likely formed during the preparation process and were retained after calcination, indicating their stability under high-temperature conditions.

### 3.2.2 Fourier-transform infrared spectroscopy

The spectrum of the synthesized catalyst was determined by FTIR to ascertain its functional group within the frequency range of 4000–500 cm<sup>-1</sup> as shown in Fig. 3. The spectra of  $\gamma$ -Al<sub>2</sub>O<sub>3</sub> demonstrated the existence of Al–O bond at wave numbers between 1750 cm<sup>-1</sup> and 2500 cm<sup>-1</sup>, where the absorption peaks between 829 cm<sup>-1</sup> and 1477 cm<sup>-1</sup> refer to the stretching vibration of Zn–O bonds. Moreover, the broad absorption peak at 3425 cm<sup>-1</sup> refers to the O–H bending vibration of adsorbed water molecules. Jafarbeigi and his friends stated that the peaks at 1050 cm<sup>-1</sup> related to Zn–O bonds and the O–H bonds of water correspond to the peaks within the range between 3200 and 3500 cm<sup>-1</sup>. They concluded that the peaks at 3468.2, 1383.79, and 535.1 cm<sup>-1</sup> appeared due to zinc oxide in ZnO/ $\gamma$ -Al<sub>2</sub>O<sub>3</sub> nanoparticles [23].

### 3.2.3 X-ray diffraction

The XRD diagrams of the synthesized ZnO/ $\gamma$ -Al<sub>2</sub>O<sub>3</sub> are shown in Fig. 4. It was observed that ZnO/ $\gamma$ -Al<sub>2</sub>O<sub>3</sub> had corresponding diffraction peaks at 2 theta ( $\theta$ ) values of 31.0°, 36.6°, 48.9°, 55.5°, 59.1°, 73.8°, and 77.2°. According to the study of Hassanzadeh-Tabrizi, it was recorded that X-ray diffraction analysis of ZnO and ZnO/ $\gamma$ -Al<sub>2</sub>O<sub>3</sub> demonstrated peaks at 2 $\theta$  values of 31.8°, 34.6°, 36.3°, 47.5°, 56.7°, and 62.9°. These results demonstrated the adsorption of ZnO on  $\gamma$ -Al<sub>2</sub>O<sub>3</sub> and ensured the presence

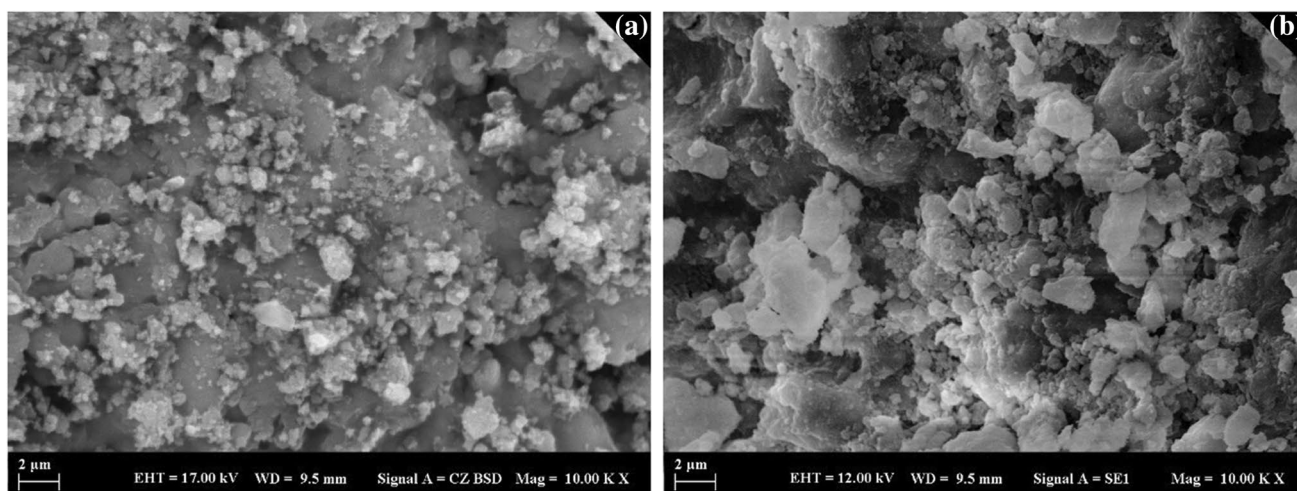


Fig. 2 SEM images: a  $\gamma$ -Al<sub>2</sub>O<sub>3</sub> and b 10 wt% ZnO/ $\gamma$ -Al<sub>2</sub>O<sub>3</sub>

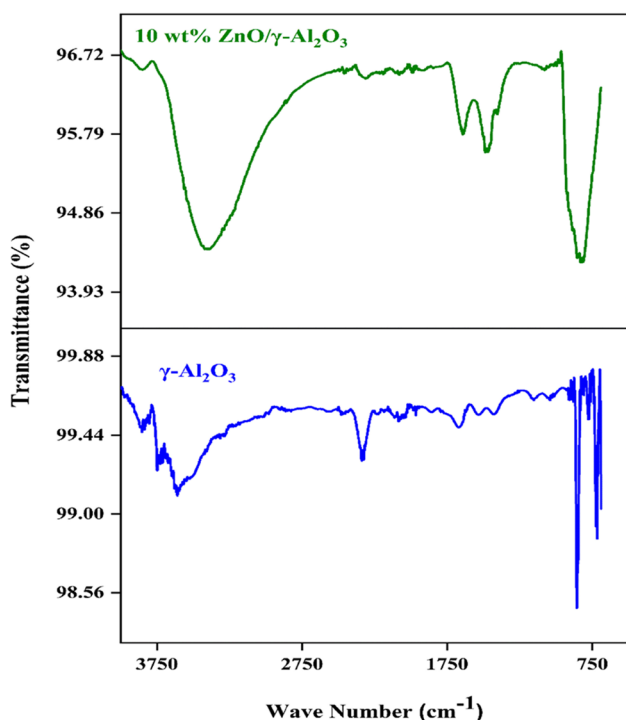


Fig. 3 FT-IR spectrum for  $\gamma$ -Al<sub>2</sub>O<sub>3</sub> and ZnO/ $\gamma$ -Al<sub>2</sub>O<sub>3</sub>

of the active sites [24]. On the other hand, it is crucial to note that the XRD peaks corresponding to bare  $\gamma$ -Al<sub>2</sub>O<sub>3</sub> exhibit low intensity in their pattern as well as in the composite's XRD pattern due to the relatively poor crystallinity of this phase in the composite. According to the Joint Committee on Powder Diffraction Standards (JCPDS) card no. (29-0063), the peaks of  $\gamma$ -Al<sub>2</sub>O<sub>3</sub> observed at  $2\theta$  values of 37.0°, 40.20°, 45.78°, 61.30°, and 66.99° were assigned to the 311, 222, 400, 511, and 440 crystal planes. These

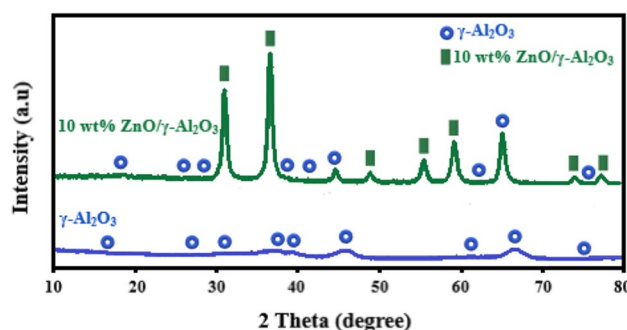
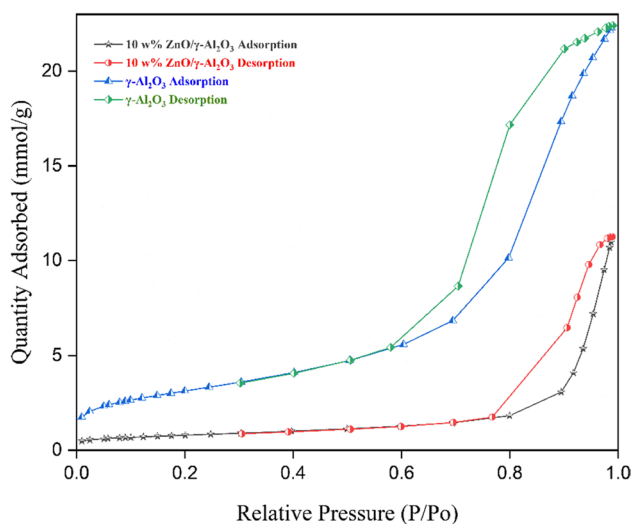


Fig. 4 XRD spectrum of  $\gamma$ -Al<sub>2</sub>O<sub>3</sub> and 10 wt% ZnO/ $\gamma$ -Al<sub>2</sub>O<sub>3</sub> catalyst

findings are consistent with the  $\gamma$ -Al<sub>2</sub>O<sub>3</sub> peaks observed in this study. Ameen et al. reported that three distinct peaks at  $2\theta$  of 37.0°, 46.0°, and 67.1° were identified during analysis, which can be attributed to the presence of the support material  $\gamma$ -Al<sub>2</sub>O<sub>3</sub>. Notably, these phases were observed with relatively low crystallinity for all the catalysts investigated [25].

### 3.2.4 Brunauer–Emmett–Teller analysis

The investigation of the specific surface area of the ZnO/ $\gamma$ -Al<sub>2</sub>O<sub>3</sub> catalyst aimed to elucidate the reduction in the total catalyst area in m<sup>2</sup>/g. The specific surface area, pore volume, and pore size distribution of  $\gamma$ -Al<sub>2</sub>O<sub>3</sub> and ZnO/ $\gamma$ -Al<sub>2</sub>O<sub>3</sub> particles were determined through nitrogen physisorption at a temperature of -195.7 °C in static mode. The N<sub>2</sub> physisorption isotherm adsorption–desorption curves of  $\gamma$ -Al<sub>2</sub>O<sub>3</sub> and ZnO/ $\gamma$ -Al<sub>2</sub>O<sub>3</sub> (Fig. 5) both exhibit type IV capillary condensation curves and H1 hysteresis loops, suggesting that the mesoporous structure



**Fig. 5** Nitrogen adsorption–desorption isotherms of  $\gamma$ - $\text{Al}_2\text{O}_3$ , and 10 wt%  $\text{ZnO}/\gamma$ - $\text{Al}_2\text{O}_3$

**Table 2** BET specific surface area, pore volume, and pore size distribution of  $\gamma$ - $\text{Al}_2\text{O}_3$  and  $\text{ZnO}/\gamma$ - $\text{Al}_2\text{O}_3$  particles

Sample	Bet surface area ( $\text{m}^2/\text{g}$ )	Pore volume ( $\text{m}^3/\text{g}$ )	Pore size (nm)
$\gamma$ - $\text{Al}_2\text{O}_3$	249	0.7768	12.26
$\text{ZnO}/\gamma$ - $\text{Al}_2\text{O}_3$	61	0.3903	24.74

of  $\gamma$ - $\text{Al}_2\text{O}_3$  was preserved after zinc oxide doping via impregnation and calcination.

Notably, unaltered  $\gamma$ - $\text{Al}_2\text{O}_3$  exhibited a larger surface area and pore volume, while the introduction of reactive zinc oxide particles into  $\gamma$ - $\text{Al}_2\text{O}_3$ , along with potential agglomeration on the support surface, resulted in a reduction in the BET surface area and pore volume, as well as an increase in pore size. These observations are presented in Table 2. In other words,  $\text{ZnO}$  occupied  $188 \text{ m}^2/\text{g}$  of  $\gamma$ - $\text{Al}_2\text{O}_3$ , resulting in a reported surface area of  $61 \text{ m}^2/\text{g}$ . According to Sulaiman et al., the addition of metal oxides to  $\gamma$ - $\text{Al}_2\text{O}_3$  obstructs the support pores, leading to a decline in the specific surface area. Despite this, the active sites in the catalyst played a crucial role in accelerating the transesterification process for biodiesel production [26].

### 3.3 Influence of reaction parameters on FAME content

During this investigation, the catalytic performance of both  $\gamma$ - $\text{Al}_2\text{O}_3$  and a 10 wt%  $\text{ZnO}/\gamma$ - $\text{Al}_2\text{O}_3$  composite was evaluated. However, the characterization of a 6 wt%  $\text{ZnO}/\gamma$ - $\text{Al}_2\text{O}_3$  catalyst was not carried out since this material was not employed in subsequent experiments and was only utilized to determine its maximum performance under critical conditions. As the

catalytic properties of the 10 wt%  $\text{ZnO}/\gamma$ - $\text{Al}_2\text{O}_3$  catalyst were found to be superior, as discussed in Sect. 3.3.1, the analysis primarily focused on this specific catalyst load.

#### 3.3.1 Effect of catalyst

The effect of catalyst usage on biodiesel yield was investigated using  $\text{ZnO}/\gamma$ - $\text{Al}_2\text{O}_3$  catalysts containing 6 wt%  $\text{ZnO}$  and 10 wt%  $\text{ZnO}$  in different oil/methanol molar ratios between 1:20 and 1:40 at a temperature of  $240 \text{ }^\circ\text{C}$ , a pressure of 9 MPa, and a residence time of 1 min. The selection of these parameters is guided by the objective of identifying the highest catalyst loading performance in a short time frame of 1 min. This is crucial because even a slight increase in performance within this brief time is significant and indicative of the catalyst's effectiveness. Therefore, the catalyst with the highest performance will be considered for further experiments. As can be seen in Fig. 6, the use of the catalyst significantly increased the biodiesel yield. With 1:40 oil/methanol mole ratio, the highest biodiesel efficiency for the 6 wt%  $\text{ZnO}/\gamma$ - $\text{Al}_2\text{O}_3$  catalyst was 61.4%, while the yield obtained for the 10 wt%  $\text{ZnO}/\gamma$ - $\text{Al}_2\text{O}_3$  catalyst was 62.4% compared to only 47.13% with no catalyst used (blank) as shown in Fig. 6. The modest rise in yield can be interpreted as an indication that the *Jatropha* oil exhibited improved conversion into fatty acid methyl esters with a catalyst loading of 10 wt%. This suggests that the catalyst loading does not contribute to any probable reverse reactions or the formation of undesirable byproducts, which may negatively impact the final yield. The experiments were conducted utilizing a varying molar ratio of oil to methanol with a 10 wt%  $\text{ZnO}/\gamma$ - $\text{Al}_2\text{O}_3$  catalyst, and the influence of other parameters was investigated.

#### 3.3.2 Effect of *Jatropha* oil/methanol molar ratio

To examine the effect of the *Jatropha* oil-to-methanol molar ratio on biodiesel yield, the reaction parameters of temperature, pressure, and time were kept constant at  $260 \text{ }^\circ\text{C}$ , 9 MPa, and 3 min, respectively. Moreover, different oil/methanol molar ratios such as 1:20, 1:25, 1:30, 1:35, and 1:40 mol/mol were applied in the presence of 10 wt%  $\text{ZnO}/\gamma$ - $\text{Al}_2\text{O}_3$  catalyst. As a result, with an oil/methanol molar ratio of 1:20, the biodiesel yield reached 83.12% as shown in Fig. 7. An increase in the oil/methanol molar ratio resulted in a higher biodiesel yield that peaked with the application of the ratio of 1:40 and reached 87.13%. These results indicate that the high solubility of methanol in the supercritical environment has a positive influence on FAME yield. In other words, the conversion of oil fatty acids into their methyl esters is enhanced in the presence of a 1:40 oil/methanol molar ratio. As the impact of increasing reaction temperature on FAME yield is notable due to enhanced molecular mobility within the reactor, further augmentations in oil/methanol

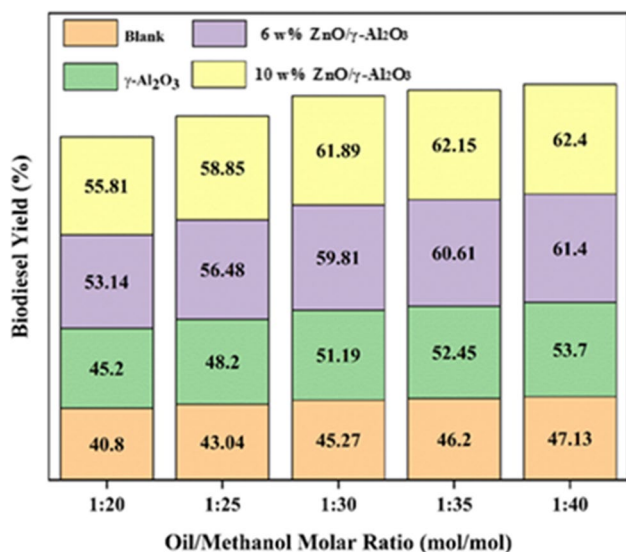


**Fig. 6** Effect of catalyst at various oil/methanol molar ratios on biodiesel yield. Reaction conditions: 240 °C reaction temperature, 9 MPa reaction pressure, 1 min residence time

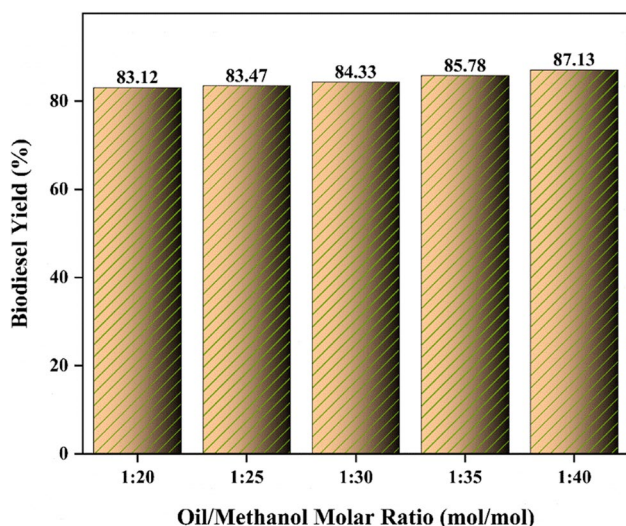


**Fig. 7** Effect of oil/methanol molar ratios on biodiesel yield. Reaction conditions: 10 wt% catalyst amount, 260 °C reaction temperature, 9 MPa reaction pressure, 3 min residence time

molar ratio are not deemed necessary. Consequently, it is more advantageous to concentrate on optimizing the reaction temperature instead of solely relying on increasing the oil/methanol molar ratio to enhance FAME yield. Makareviciene and Sendzikiene reported that under supercritical conditions, biodiesel synthesis yields a high ester yield with a higher oil-to-alcohol molar ratio [27]. Sawiwat and Kajorncheappunngam reported that the FAME content was increased from 81.49 to 87.54% by increasing the molar ratio of oil to methanol from 1:20 to 1:40. Moreover, the

increased FAME content was attributed to the surroundingness of the oil molecules by supercritical methanol, which resulted in a high solubility due to the high interactions between the oil and methanol [28]. Singh et al. mentioned that there was no significant biodiesel yield by increasing of alcohol-to-oil molar ratio in supercritical transesterification more than 1:40. They justified the decrease in biodiesel yield by increasing the heating load, which consequently reduces the temperature of the reaction mixture [29].

### 3.3.3 Effect of the reaction temperature

To increase the biodiesel produced after 3 min at 260 °C above 87.13%, the temperature parameters of 280 °C and 300 °C were investigated, while the oil-to-methanol molar ratio was kept constant at 1:40. Under these conditions, it was found that the biodiesel yield increased slowly (88.27%) when the temperature was increased from 260 °C to 280 °C and significantly (95.64%) when 300 °C was applied (Fig. 8). As the reaction temperature increased, there was a clear impact on the interactions between oil and methanol molecules. This effect implies that higher temperatures enhance the intermolecular associations between these components. Additionally, the observed increase in the yield of FAME suggests that the current methanol ratio is satisfactory and does not necessitate any further augmentation, in accordance with our previous discussion. Karki et al. mentioned that temperature has an important role in supercritical alcohol transesterification to obtain biodiesel. They concluded that as the temperature increases, the O–H bonds decrease and the alcohol's polarity decreases leading to further reaction [30].

### 3.3.4 Effect of the residence time

To determine the optimal reaction time, experiments performed at 1 min were analyzed. The results revealed sub-standard transesterification efficiency and little increase in yield by (65.25%, 65.51%, and 65.83%) at 260 °C, 280 °C, and 300 °C, respectively. The results obtained after 3 min of reaction time at 300 °C were compared with those obtained after reaction durations of 5, 7, and 9 min (Fig. 9). As the reaction time increased, the total yield also increased, with gains of 1.96%, 4.25%, and 4.36% recorded at 5, 7, and 9 min, respectively.

Based on the findings, the optimal biodiesel yield for high temperature and reaction time was achieved after 3 min of reaction time. The yield increases to above 95% after this time, which is very close to the final yield of 100% achieved after 9 min. Therefore, it can be concluded that a shorter reaction time of 3 min can result in a near-complete conversion of FAME, making it a more efficient and cost-effective process compared to the longer reaction time of 9 min. Moreover, the increase in reaction temperature and oil-to-methanol molar ratio under supercritical methanol

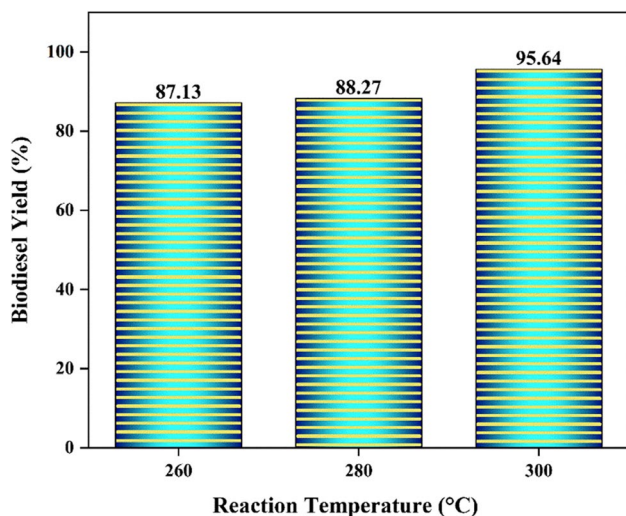


**Fig. 8** Effect of reaction temperature on biodiesel yield. Reaction conditions: 1:40 oil-to-methanol molar ratio, 10 wt% catalyst amount, 9 MPa reaction pressure, and 3 min residence time

conditions is associated with a higher degree of molecular motion and improved solubility of reactants, respectively. As the yields obtained at a reaction temperature of 300 °C and an oil to methanol molar ratio of 1:40 exceeded 95%, further investigation into higher temperature and molar ratio values was deemed unnecessary. The sample was subsequently analyzed by GC–MS, as shown in Fig. 10, and the error ( $\delta = 0.017$ ) was calculated.

In the following, a comparison of heterogeneous catalysts containing ZnO for biodiesel production with different raw materials reported in the literature is presented in Table 2.

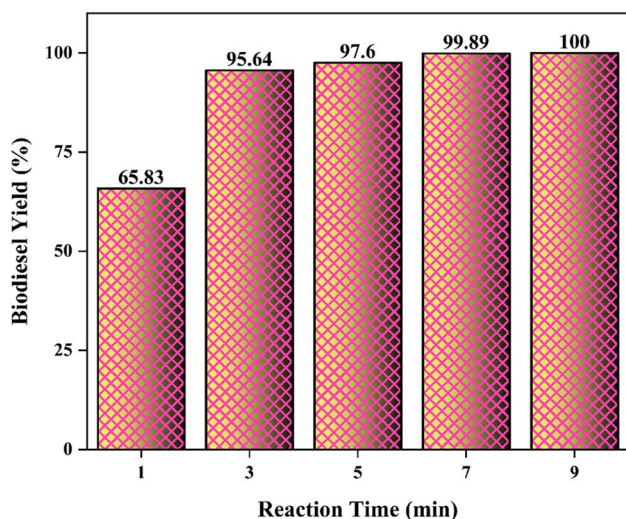


**Fig. 9** Effect of residence time on biodiesel yield. Reaction conditions: 1:40 oil-to-methanol molar ratio, 10 wt% catalyst amount, 300 °C reaction temperature, 9 MPa residence pressure

As evident, a considerable study has investigated the effect of ZnO catalyst on biodiesel production by applying different crude oil sources under different reaction parameters. In this work, the use of inedible *Jatropha* as a crude oil in biodiesel production gives priority to consider its commercial implementation. Moreover, although lanthanum oxide was used alongside zinc oxide in the study of Mazzanov et al., the yield was 65.54% lower compared to the yield of this study [31]. In addition, the reaction time of 5 h was very long compared to 3 min in our study. Similarly, other studies required 3 h, 5 h, and 6 h to achieve biodiesel yields of 99.0%, 95.7%, and 92.29%, respectively [32–34]. On the other hand, Saez et al. studies were compiled using a short reaction time of 4 min, but biodiesel production was also 15.94% and 19.65% lower than that achieved in this work when applying ZnO and ZnO-La<sub>2</sub>CO<sub>3</sub>, respectively [35]. Except where noted, the reaction time of Wan et al. was 1 h, considering their use of edible soybean oil, indicating lower selectivity for commercial application [36].

Although the supercritical studies of Al-Saadi et al. and Hoang et al. achieved high yields of biodiesel, the reaction times were too long [33, 37]. Good design and optimum selection of the reactor are the most important factors for obtaining high yields of biodiesel. As in this work, the high yield in a short reaction time may be attributed to the rapid interaction between the oil and methanol molecules when continuously pumped into the catalyst filled PBR under supercritical conditions, ensuring the maximum possible conversion of oil into biodiesel. As concluded, for catalysts applied under supercritical conditions and other technologies, the reaction time column presents the success of our work to reduce the reaction time to 3 min according to the stated parameters, which

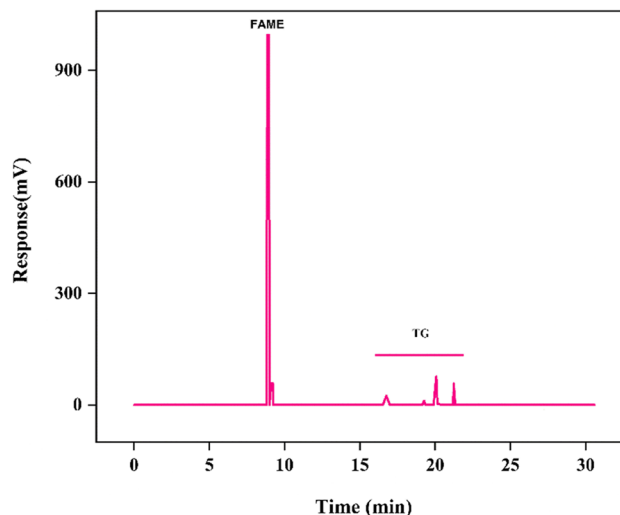


**Fig. 10** Chromatogram of biodiesel with high FAMES%. Sample conditions: 1:40 oil-to-methanol molar ratio, 10 wt% catalyst amount, 300 °C reaction temperature, 9 MPa reaction pressure, and 3 min residence time



**Table 3** Comparison of heterogeneous catalysts containing ZnO with different raw materials for biodiesel production

Oil/alcohol molar ratio (mol/mol)	Catalyst	Calcination (°C/h)	Reaction temperature (°C)	Reaction pressure (MPa)	Reaction time (min)	Yield (%)	Ref
Rapeseed/EtOH 1:12	5% ZnO/Al <sub>2</sub> O <sub>3</sub>	500/4	350	30	30	97.45	[31]
Waste oil/MeOH 1:12.6	3:1 ZnO–La <sub>2</sub> CO <sub>3</sub>	450/8	200	–	180	99.0	[32]
Cooking oil/EtOH 1:10	SrO–ZnO/Al <sub>2</sub> O <sub>3</sub>	900/6	75	–	300	95.7	[33]
Kesambi/MeOH 1:12	4% ZnO/Al <sub>2</sub> O <sub>3</sub>	500/6	65	–	360	92.29	[34]
Vegetable oil/MeOH–CO <sub>2</sub> 1:25	ZnO	500/5	200	20	4	79.7	[35]
Vegetable oil/MeOH–CO <sub>2</sub> 1:25	1:1 ZnO–La <sub>2</sub> CO <sub>3</sub>	500/5	200	20	4	76	[35]
Soybean/MeOH 1:18	4% MnO <sub>3</sub> –ZnO	300/0.5	175	10	60	94.2	[36]
Rapeseed/EtOH 1:42	4% ZnO	200/2	270	15	60	93	[37]
Rapeseed/MeOH 1:40	3% ZnO	–	250	35	10	96.88	[38]
Jatropha/MeOH 1:6	La <sub>2</sub> O <sub>3</sub> –ZnO	550/3	60	–	300	30.1	[39]
Rapeseed/MeOH 1:40	1% ZnO	800/5	250	10.5	10	95	[40]
Jatropha/MeOH 1:40	10% ZnO/γ–Al <sub>2</sub> O <sub>3</sub>	900/4	300	9	3	95.64	This work

will be a credit for achieving high content and quantity of biodiesel. Upon closer examination of Table 3, it becomes apparent that the results of these studies are closely related to the specific parameters employed in each investigation. Factors such as the type of raw material, catalyst loading amount, catalyst with or without a supporter, oil-to-methanol molar ratio, and whether the reaction is conducted under supercritical alcohol conditions all play a role. Additionally, the selection of reactor type can impact the results, as a complete reaction may occur earlier than the set reaction time in a batch reactor. Given the careful selection of parameters in this work, the optimal conditions presented are a testament to its success and reflect the importance of considering all relevant factors in biodiesel production.

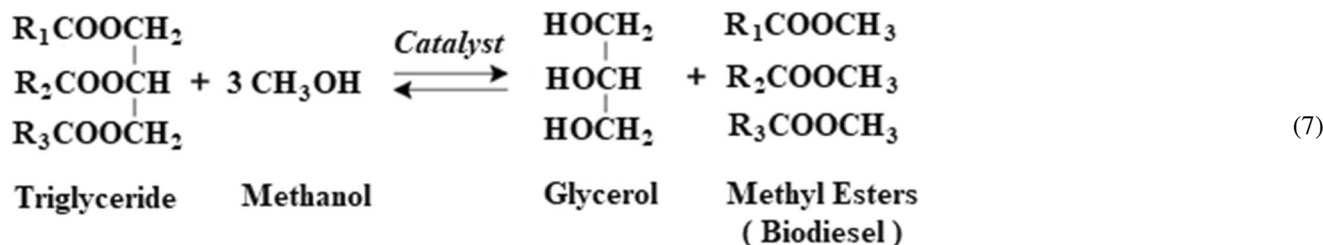
The reusability of the ZnO/γ–Al<sub>2</sub>O<sub>3</sub> catalyst was investigated over six rounds to assess the catalyst's activity in each round, with the biodiesel yield percentage being reported (Fig. 11a). The results indicated that after six rounds, the yield percentage decreased by 0.48%. Furthermore, the FTIR spectra of the reused catalyst were compared to those of the bare and loaded γ–Al<sub>2</sub>O<sub>3</sub>, as depicted in Fig. 11b. Notably, the peaks in the spectrum of the reused catalyst collapsed due to the presence of oil contamination, which affected the shape of the spectrum. However, despite this, the peaks based on wave numbers still indicated that the

catalyst remained active. This suggests that the γ–Al<sub>2</sub>O<sub>3</sub> support still retained its catalytic properties to some extent.

### 3.4 Kinetic calculations and appropriate reaction rate

Supercritical methanol transesterification is a molecular-level chemical reaction that replaces one ester group with another using methanol as the reaction medium under high pressure and temperature. The catalyst breaks the bonds between the oxygen atom and the carbonyl carbon atom in the ester group of oil, forming an unstable and highly nucleophilic alkoxide ion [41]. The alkoxide ion then reacts with the alcohol molecule, forming a new ester bond and releasing the original alcohol molecule as a byproduct. The resultant product is a new ester molecule with a different alcohol group attached, offering advantages such as increased reaction rates and selectivity.

The conversion of triglycerides in CJCO with methanol into biodiesel and glycerol is achieved by reaction mechanism shown in Eq. (7) at supercritical conditions of the reactant methanol, and the reaction occurs very quickly without being subject to any limitations. The reaction tends to be irreversible, and the equilibrium is discernibly towards the product side.



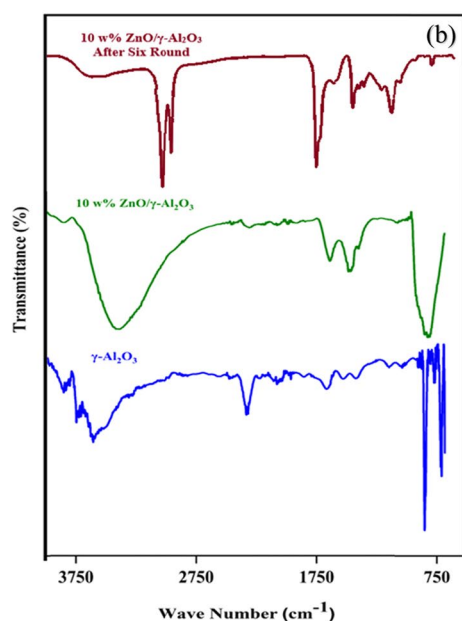
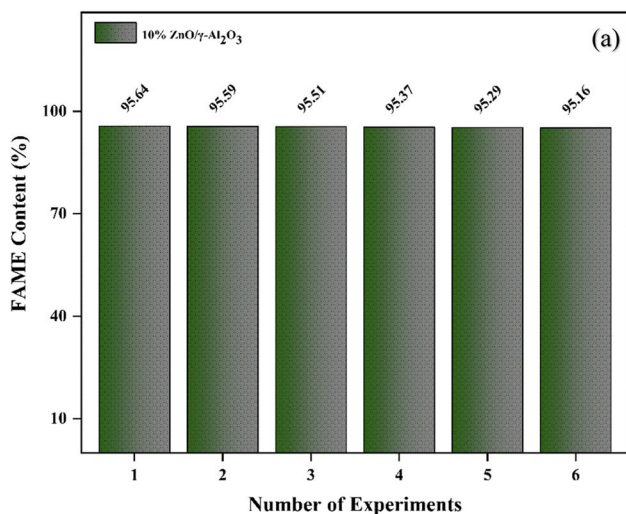


**Fig. 11** **a** Catalyst reuse, and **b** FTIR of reused catalyst

To understand the kinetics of transesterification of a 10 wt% ZnO/ $\gamma$ -Al<sub>2</sub>O<sub>3</sub> catalyst at different residence times, temperatures, and molar ratios of oil/methanol, a kinetic model was proposed and then compared with the experimentally obtained biodiesel yield results. Mathematically, the appropriate rate equation for the reaction with respect to the reactants (jatropha oil and MeOH) can be written as:

$$-\frac{d[C_{oil}]}{d\tau} = k_0 \times e^{-\frac{E_a}{R\tau}} \times [C_{oil}]^a \times [C_{MeOH}]^b \quad (8)$$

Since there is an excess of methanol in the system, the change in MeOH concentration is negligible and the value of  $b$  in Eq. (8) can be considered 0. Accordingly, by rearranging the above equation, the total kinetic equation that

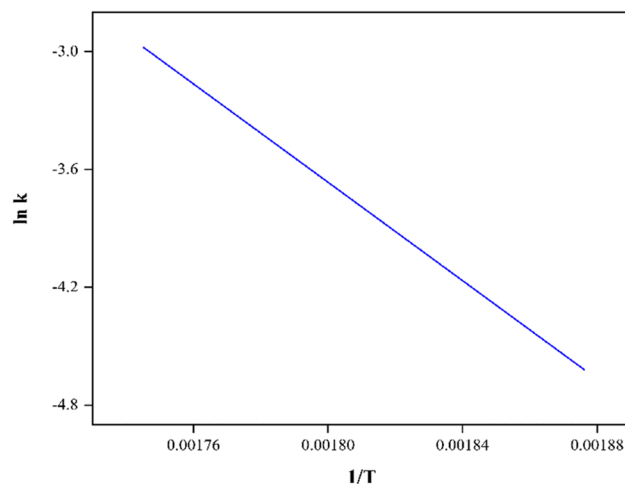


**Fig. 12** Relationship between the reaction rate constant and temperature

depends only on the change in oil concentration in terms of oil conversion ( $X$ ) can be written as in Eq. (9):

$$\frac{dX}{d\tau} = k_0 \times e^{-\frac{E_a}{R\tau}} \times [C_{oil,0}]^{a-1} \times (1-X)^a \quad (9)$$

$$X = 1 - [1 + (a-1) \times k_0 \times e^{-\frac{E_a}{R\tau}} \times [C_{oil,0}]^{a-1} \times \tau]^{\frac{1}{1-a}} \quad (10)$$

Data obtained from the experiments were substituted into Eq. (10) and subjected to nonlinear regression analysis using the Statistica package software. The kinetic data ( $\alpha$ ,  $k_0$ ,  $E_a$ ) were calculated and the appropriate reaction model was proposed within a 5% deviation rate for the experimental data according to the proposed reaction model. According to this model, the appropriate values of the

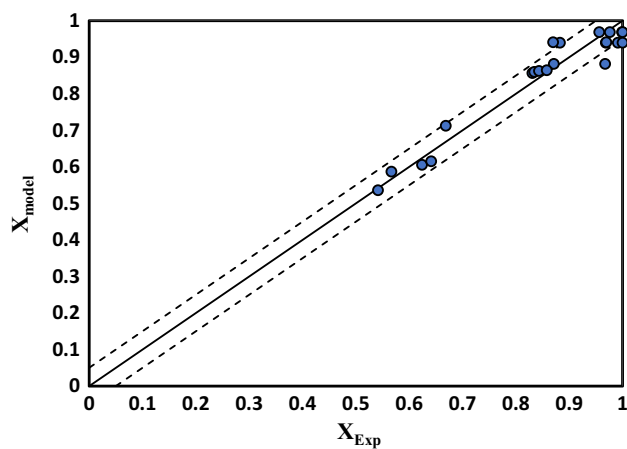


**Fig. 13** Comparison between the predicted and experimental oil conversions

reaction degree ( $\alpha$ ), Arrhenius constant ( $k_0$ ), and the activation energy ( $E_a$ ) were obtained as 2.24,  $1.63 \times 10^8 \text{ L}^{1.24}/\text{mol}^{1.24} \text{ min}$  and 104.28 kJ/mol, respectively ( $r^2 = 0.9662$ ). In addition, the activation energy of the chemical reaction being studied is confirmed by acquiring the relationship between the reaction rate constant and temperature as presented in Fig. 12.

A comparison between the predicted and experimental oil conversions is shown in Fig. 13, and it can be said that the proposed model fits satisfactorily with our experimental data. The above values were applied in the final reaction rate equation, and the overall equation for the experiments was written as follows (Eq. 11):

$$-\frac{dC_{oil}}{d\tau} = 1.63 \cdot 10^8 \left( \frac{L^{1.24}}{\text{mol}^{1.24} \cdot \text{min}} \right) \cdot e^{-\frac{104.28(\text{kJ/mol})}{RT}} \cdot C_{oil}^{2.24} \quad (11)$$

## 4 Conclusion

The present study investigated the production of biodiesel from *Jatropha* oil using ZnO/ $\gamma$ -Al<sub>2</sub>O<sub>3</sub> as a heterogeneous catalyst. The results showed that the use of 10 wt% ZnO/ $\gamma$ -Al<sub>2</sub>O<sub>3</sub> significantly increased the biodiesel yield compared to the reaction without catalyst. Under optimal conditions of a molar ratio of 1:40 oil/methanol, a reaction temperature of 300 °C, a reaction pressure of 9 MPa, and a residence time of 3 min, a yield of 95.64% was obtained. The use of the heterogeneous catalyst reduced the reaction time to 3 min compared to conventional reaction times of hours. This study suggests an appropriate kinetic rate equation based on experimental results, indicating that the reaction rate increases with increasing temperature and methanol molar ratio. These findings are useful in optimizing reaction conditions for biodiesel production through supercritical alcohol transesterification, which is the main reaction used to convert crude *jatropha* oil into biodiesel.

**Acknowledgements** We are grateful to Yildiz Technical University Research Fund for their support.

**Author contribution** Zeliha Derya Ceran: methodology, formal analysis, investigation and writing the original draft. Velid Demir: catalyst synthesis and characterization, conceptualization, methodology, formal analysis investigation, writing and reviewing the original draft. Mesut Akgün: supervision, funding acquisition, writing—review and editing.

**Funding** Open access funding provided by the Scientific and Technological Research Council of Türkiye (TÜBİTAK). This research is supported by grant number FBA-2020–3736 from Yildiz Technical University, Department of Scientific Research Project Coordination.

**Data availability** Not applicable.

## Declarations

**Ethical approval** Not applicable.

**Competing interests** The authors declare no competing interests.

**Open Access** This article is licensed under a Creative Commons Attribution 4.0 International License, which permits use, sharing, adaptation, distribution and reproduction in any medium or format, as long as you give appropriate credit to the original author(s) and the source, provide a link to the Creative Commons licence, and indicate if changes were made. The images or other third party material in this article are included in the article's Creative Commons licence, unless indicated otherwise in a credit line to the material. If material is not included in the article's Creative Commons licence and your intended use is not permitted by statutory regulation or exceeds the permitted use, you will need to obtain permission directly from the copyright holder. To view a copy of this licence, visit <http://creativecommons.org/licenses/by/4.0/>.

## References

- Nayab R, Imran M, Ramzan M, Tariq M, Taj MB, Akhtar MN, Iqbal HMN (2022) Sustainable biodiesel production via catalytic and non-catalytic transesterification of feedstock materials – a review. *Fuel* 328:125254. <https://doi.org/10.1016/j.fuel.2022.125254>
- Roman-Figueroa C, Olivares-Carrillo P, Paneque M, Palacios-Nereo FJ, Quesada-Medina J (2016) High-yield production of biodiesel by non-catalytic supercritical methanol transesterification of crude castor oil (*Ricinus communis*). *Energy* 107:165–171. <https://doi.org/10.1016/j.energy.2016.03.136>
- Lee HS, Seo H, Kim D, Lee YW (2020) One-pot supercritical transesterification and partial hydrogenation of soybean oil in the presence of Pd/Al<sub>2</sub>O<sub>3</sub> or Cu or Ni catalyst without H<sub>2</sub>. *J Supercrit Fluids* 156:104683. <https://doi.org/10.1016/j.supflu.2019.104683>
- Yaakob Z, Mohammad M, Alherbawi M, Alam Z, Sopian K (2013) Overview of the production of biodiesel from waste cooking oil. *Renew Sustain Energy Rev* 18:184–193. <https://doi.org/10.1016/j.rser.2012.10.016>
- Semwal S, Arora AK, Badoni RP, Tuli DK (2011) Biodiesel production using heterogeneous catalysts. *Bioresour Technol* 102:2151–2161. <https://doi.org/10.1016/j.biortech.2010.10.080>
- Zhang J, Chen S, Yang R, Yan Y (2010) Biodiesel production from vegetable oil using heterogeneous acid and alkali catalyst. *Fuel* 89:2939–2944. <https://doi.org/10.1016/j.fuel.2010.05.009>
- Demir V, Akgün M (2022) New catalysts for biodiesel production under supercritical conditions of alcohols: a comprehensive review. *ChemistrySelect* 7:e202104459. <https://doi.org/10.1002/slct.202104459>
- Ramos M, Dias APS, Puna JF, Gomes J, Bordado JC (2019) Biodiesel production processes and sustainable raw materials. *Energies* 12(23):4408. <https://doi.org/10.3390/en12234408>
- Micic RD, Tomić MD, Kiss FE, Nikolić-Djorić EB, Simikić M (2014) Influence of reaction conditions and type of alcohol on biodiesel yields and process economics of supercritical transesterification. *Energy Convers Manag* 86:717–726. <https://doi.org/10.1016/j.enconman.2014.06.052>
- Tan KT, Gui MM, Lee KT, Mohamed AR (2011) Supercritical alcohol technology in biodiesel production: a comparative study between methanol and ethanol. *Energy Sources, Part A: Recover*

- Util Environ Eff 33:156–163. <https://doi.org/10.1080/15567030902937226>
11. Bernal JM, Lozano P, García-Verdugo E, Burguete MI, Sánchez-Gómez G, López-López G, Pucheault M, Vaultier M, Luis SV (2012) Supercritical synthesis of biodiesel. *Molecules* 17:8696–8719. <https://doi.org/10.3390/molecules17078696>
  12. Deshpande SR, Sunol AK, Philippidis G (2017) Status and prospects of supercritical alcohol transesterification for biodiesel production. *Wiley Interdiscip Rev Energy Environ* 6:e252. <https://doi.org/10.1002/wene.252>
  13. Chauhan BS, Kumar N, Cho HM (2012) A study on the performance and emission of a diesel engine fueled with Jatropha biodiesel oil and its blends. *Energy* 37:616–622. <https://doi.org/10.1016/j.energy.2011.10.043>
  14. Pradhan S, Naik SN, Khan MI, Sahoo PK (2012) Experimental assessment of toxic phytochemical in Jatropha curcas: oil, cake, bio-diesel and glycerol. *J Sci Food Agric* 92(3):511–519. <https://doi.org/10.1002/jsfa.4599>
  15. Achten WMJ, Mathijs E, Verchot L, Singh VP, Aerts R, Muys B (2007) Jatropha biodiesel fueling sustainability? *Biofuels Bioprod Biorefin* 1:283–291. <https://doi.org/10.1002/bbb.39>
  16. Lifang W, Goh ML, Tian D, Gu K, Hong Y, Yin Z (2017) Isolation and characterization of curcumin genes with distinct expression patterns in leaves and seeds of Jatropha curcas L. *Plant Gene* 9:34–44. <https://doi.org/10.1016/j.plgene.2016.12.005>
  17. Abdullah BM, Yusop RM, Salimon J, Yousif E, Salih N (2013) Physical and chemical properties analysis of jatropha curcas seed oil for industrial applications. *Int J Chem Mol Nuc Mater Metal Eng* 7:893–896
  18. Aleman-Ramirez JL, Reyes-Vallejo O, Okoye PU, Sanchez-Albores R, Maldonado-Álvarez A, Sebastian PJ (2023) Crystal phase evolution of high temperature annealed Fe<sub>3</sub>O<sub>4</sub>-CaO catalysts for biodiesel production. *Biofuels Bioprod Bioref* 17:843–858. <https://doi.org/10.1002/bbb.2478>
  19. Freitas SVD, Silva EFA, Pastoriza-Gallego MJ, Piñeiro MM, Lima AS, Coutinho JAP (2013) Measurement and prediction of densities of vegetable oils at pressures up to 45 MPa. *J Chem Eng Data* 58:3046–3053. <https://doi.org/10.1021/jc400474w>
  20. Peng D, Robinson DB (1976) A new two-constant equation of state. *Ind Eng Chem Fundam* 15:59–64. <https://doi.org/10.1021/i160057a011>
  21. Kumar R, Das N (2018) Seed oil of Jatropha curcas L. germplasm: analysis of oil quality and fatty acid composition. *Ind Crops Prod* 124:663–668. <https://doi.org/10.1016/j.indcrop.2018.08.031>
  22. Riayatsyah TM, Sebayang AH, Silitonga AS, Padli Y, Fattah IM, Kusumo F, Ong HC, Mahlia TM (2022) Current progress of jatropha curcas commoditisation as biodiesel feedstock: a comprehensive review. *Frontiers Energy Res* 9:815416. <https://doi.org/10.3389/fenrg.2021.815416>
  23. Jafarbeigi E, Ahmadi Y, Mansouri M, Ayatollahi S (2022) Experimental core flooding investigation of new ZnO- $\gamma$ -Al<sub>2</sub>O<sub>3</sub> nanocomposites for enhanced oil recovery in carbonate reservoirs. *ACS Omega* 7:39107–39121. <https://doi.org/10.1021/acsomega.2c04868>
  24. Hassanzadeh-Tabrizi SA (2017) Synthesis and characterization of nano Ce doped ZnO/ $\gamma$ -Al<sub>2</sub>O<sub>3</sub> with improved photocatalytic activity. *J Mat Sci: Mat in Elect* 28:9528–9534. <https://doi.org/10.1007/s10854-017-6698-8>
  25. Ameen M, Azizan MT, Ramli A, Yusup S, Abdullah B (2020) The effect of metal loading over Ni/ $\gamma$ -Al<sub>2</sub>O<sub>3</sub> and Mo/ $\gamma$ -Al<sub>2</sub>O<sub>3</sub> catalysts on reaction routes of hydrodeoxygenation of rubber seed oil for green diesel production. *Catal Today* 355:51–64. <https://doi.org/10.1016/j.cattod.2019.03.028>
  26. Sulaiman NF, Lee SL, Toemen S, Bakar WA (2020) Physicochemical characteristics of Cu/Zn/ $\gamma$ -Al<sub>2</sub>O<sub>3</sub> catalyst and its mechanistic study in trans-esterification for biodiesel production. *Renew Energy* 156:142–157. <https://doi.org/10.1016/j.renene.2020.04.021>
  27. Makareviciene V, Sendzikiene E (2021) Noncatalytic biodiesel synthesis under supercritical conditions. *Processes* 9:138. <https://doi.org/10.3390/pr9010138>
  28. Sawiwat T, Kajorncheappunngam S (2015) Biodiesel production from crude rubber seed oil using supercritical methanol transesterification. *App Mech Mater* 781:655–658. <https://doi.org/10.4028/www.scientific.net/AMM.781.655>
  29. Singh CS, Kumar N, Gautam R (2021) Supercritical transesterification route for biodiesel production: effect of parameters on yield and future perspectives. *Environ Prog Sustain Energy* 40:e13685. <https://doi.org/10.1002/ep.13685>
  30. Karki S, Sanjel N, Poudel J, Choi JH, Oh SC (2017) Supercritical transesterification of waste vegetable oil: characteristic comparison of ethanol and methanol as solvents. *App Sci* 7:632. <https://doi.org/10.3390/app7060632>
  31. Mazanov SV, Gabitova AR, Usmanov RA, Gumerov FM, Labidi S, Amar MB, Passarello JP, Kanaev A, Volle F, Neindre BL (2016) Continuous production of biodiesel from rapeseed oil by ultrasonic assist transesterification in supercritical ethanol. *J Supercrit Fluids* 118:107–118. <https://doi.org/10.1016/j.supflu.2016.07.009>
  32. Yan S, Salley SO, Simon Ng KY (2009) Simultaneous transesterification and esterification of unrefined or waste oils over ZnO-La<sub>2</sub>O<sub>3</sub> catalysts. *Appl Catal A Gen* 353:203–212. <https://doi.org/10.1016/j.apcata.2008.10.053>
  33. Al-Saadi A, Mathan B, He Y (2020) Biodiesel production via simultaneous transesterification and esterification reactions over SrO-ZnO/Al<sub>2</sub>O<sub>3</sub> as a bifunctional catalyst using high acidic waste cooking oil. *Chem Eng Res Design* 162:238–248. <https://doi.org/10.1016/j.cherd.2020.08.018>
  34. Asri NP, Soe'eib S, Poedjono B, Suprpto (2018) Alumina supported zinc oxide catalyst for production of biodiesel from kesambi oil and optimization to achieve highest yields of biodiesel. *Euro-Mediterr. J Environ Integr* 3:3. <https://doi.org/10.1007/s41207-017-0043-8>
  35. Saez B, Santana A, Ramírez E, Macaira J, Ledesma C, Llorca J, Larrayoz MA (2014) Vegetable oil transesterification in supercritical conditions using co-solvent carbon dioxide over solid catalysts: a screening study. *Energy Fuels* 28:6006–6011. <https://doi.org/10.1021/ef5006786>
  36. Wan L, Liu H, Skala D (2014) Biodiesel production from soybean oil in subcritical methanol using MnCO<sub>3</sub>/ZnO as catalyst. *App Catal B: Environ* 152–153:352–359. <https://doi.org/10.1016/j.apcatb.2014.01.033>
  37. Hoang D, Bensaid S, Saracco G, Pirone R, Fino D (2017) Investigation on the conversion of rapeseed oil via supercritical ethanol condition in the presence of a heterogeneous catalyst. *Green Process Synth* 6:91–101. <https://doi.org/10.1515/gps-2016-0081>
  38. Kim M, Lee HS, Yoo SJ, Youn YS, Shin YH, Lee YW (2013) Simultaneous synthesis of biodiesel and zinc oxide nanoparticles using supercritical methanol. *Fuel* 109:279–284. <https://doi.org/10.1016/j.fuel.2012.12.055>
  39. Endalew AK, Kiros Y, Zanzi R (2011) Heterogeneous catalysis for biodiesel production from Jatropha curcas oil (JCO). *Energy* 36:2693–2700. <https://doi.org/10.1016/j.energy.2011.02.010>
  40. Yoo SJ, Lee HS, Veriansyah B, Kim J, Kim JD, Lee YW (2010) Synthesis of biodiesel from rapeseed oil using supercritical methanol with metal oxide catalysts. *Bioresour Tech* 101:8686–8689. <https://doi.org/10.1016/j.biortech.2010.06.073>
  41. Patel NK, Shah SN (2015) Biodiesel from plant oils. In: Ahuja S (ed) *Food, energy, and water: The chemistry connection*. Elsevier, Amsterdam, pp 277–307. <https://doi.org/10.1016/B978-0-12-800211-7.00011-9>

**Publisher's Note** Springer Nature remains neutral with regard to jurisdictional claims in published maps and institutional affiliations.